Separation Science and Technology
Publication details, including instructions for authors and subscription information:
http://www.informaworld.com/smpp/title~content=t713708471

Modelling the Effect of Particle Size in Microfiltration

D. Gassara[a]; P. Schmitz[b]; A. Ayadi[a]; M. Prat[c]
[a] LRAE ENIS Sfax, Tunisie [b] LISBP UMR 5504 UMR 792 CNRS INRA INSA, Toulouse, France [c] IMFT UMR CNRS 5502, Toulouse, France

To cite this Article Gassara, D. , Schmitz, P. , Ayadi, A. and Prat, M.(2008) 'Modelling the Effect of Particle Size in Microfiltration', Separation Science and Technology, 43: 7, 1754 — 1770
To link to this Article: DOI: 10.1080/01496390801973755
URL: http://dx.doi.org/10.1080/01496390801973755

Separation Science and Technology, 43: 1754–1770, 2008

ISSN 0149-6395 print/1520-5754 online
DOI: 10.1080/01496390801973755

Modelling the Effect of Particle Size in Microfiltration

D. Gassara,[1] P. Schmitz,[2] A. Ayadi,[1] and M. Prat[3]

[1]LRAE ENIS Sfax, Tunisie
[2]LISBP UMR 5504 UMR 792 CNRS INRA INSA, Toulouse, France
[3]IMFT UMR CNRS 5502, Toulouse, France

Abstract: Particle deposition at the filter surface in microfiltration is studied to better understand the effect of particle size on cake morphology and permeability reduction. Numerical simulations are carried out on a Hele Shaw cell which consists of a representative unit element of a two dimensional spatially periodic flat plate with pores. The particle concentration in the fluid is assumed to be low so that particles enter one by one into the computation domain. Particles follow the flow streamlines under creeping flow conditions from a random initial location until they are subjected to physico-chemical interactions near the filter surface or a particle already deposited. The computational domain consists of two regions: a fluid region and a porous medium region, i.e. the particle cake. The flow over the two regions of the Hele Shaw cell is computed using the Darcy model, including the variations of the permeability field due to the cake formation. Results show that both the permeability and the filtration efficiency are affected significantly by particle size.

Keywords: Particle, size, filtration, cake, Darcy, deposition

INTRODUCTION

Microfiltration is a solid-liquid separation process widely used in applications such as water clarification, or by the chemical and mineral industries. During separation, suspended particles are convected towards the filter and are eventually captured at the filter surface causing a drastic increase of the local

Received 25 September 2007, Accepted 12 January 2008
Address correspondence to P. Schmitz, LISBP UMR 5504 UMR 792 CNRS INRA INSA, Toulouse, France. E-mail: schmitz@insa-toulouse.fr

concentration of particles, gradual fouling and consequent permeability reduction. Experiments show the formation of a cake layer which is finally responsible for the abrupt mass flux decline with time (1, 2). A lot of models have been proposed to simulate mass flux decline with time for various experimental conditions. Some of them focused on the effect of particle size on filtration performance (3, 4). The classical empirical laws proposed to predict mass flux decline and/or pressure drop increase with time of operation consider the filter as a smooth surface with suction boundary conditions (5–7). In addition the cake layer is also assumed to be homogeneous, its permeability being equal to its intrinsic permeability which can be calculated for instance using a simple law such as the Carman Kozeny law. However, from a theoretical point of view, the problem of the apparent permeability evolution of the cake remains largely open. On the one hand, there is a rupture of space periodicity of the flow within the porous medium, i.e. the cake, in the vicinity of the filter surface. On the other hand, there is no separation of the scales when the particle size and the pore size are of the same order of magnitude. Moreover, the "local" permeability, i.e. the permeability on a Representative Elementary Volume of the aforementioned porous medium, depends on the complex microstructure, resulting from particle arrangement in the cake, which varies according to the hydrodynamic and physicochemical interactions between particles and walls (other particles and filter surface).

A number of models have already been developed to simulate particle accumulation at the filter surface taking into account the discrete geometry of the filter surface (wall and pores). Pioneer works of Schmitz et al. (8) considered ballistic deposition of monosized particles on a 2D spatially periodic model membrane. Physico-chemical interactions were taken into account using empirical capture rules. Specific deposit microstructures, qualitatively in good agreement with experimental observations, were obtained. The work of Frey and Schmitz (9) was specially focused on the effect of hydrodynamic interactions, i.e. viscous repulsion, on particle trajectory. A capture distance was considered to model physico-chemical interactions. The particle capture distribution function at the model filter surface for different parameters such as particle size, pore size and fluid flow conditions clearly showed the prevalent location of the first particle deposited. However, it was not possible to deduce information on cake growth and subsequent permeability reduction. Seminario et al. (10) studied the particle capture at the membrane surface with experiments and Monte Carlo simulations. Particle capture and size exclusion at pore segments were considered as the dominant mechanisms of membrane fouling. Chang et al. (11) did experiments with latex beads to study the effect of particle size and particle size distribution function on the permeate flux of cross flow microfiltration. The work of Dufreche et al. (12) was dedicated to the apparent permeability of a porous layer backed by a perforated plate, i.e. the case when there is a separation of the scales, meaning that the particle size is one or several order of magnitude

lower than the pore size of the filter surface. Some laws of permeability variations as a function of cake thickness and pore size were given. Another study dedicated to the case when there is no separation of the scales was performed on square arrangements of monosized particles as a model of cake (Dufreche et al. (13)). Recently, Noel (14) performed numerical simulations of particle accumulation and cake formation in three dimensions (3D) using the Darcy Brinkman model to calculate fluid flow in both fluid and porous domain. The influence of particle size and pore size on the variations of macroscopic parameters, such as permeability, average compactness of the deposit and filtration efficiency as a function of the volume of deposited particles, was presented but physico-chemical interactions were neglected because of computer time requirements. In all these works it was shown that the discrete geometry of the filter surface had a significant impact on particle deposition, cake morphology and subsequent permeability reduction, in particular at the beginning of the filtration process, i.e. at the very first steps of cake formation. But all these works consider only separately but not together the two main mechanisms responsible for particle capture and cake formation, which are hydrodynamic and physico-chemical interactions.

In the present work, the deposition of spherical particles at the filter surface in microfiltration is studied to better understand the effect of particle size on cake morphology, permeability reduction, and capture efficiency. Numerical simulations are carried out on a Hele Shaw cell which consists of a representative unit element of a two dimensional spatially periodic flat plate with pores. Particle concentration in the fluid is assumed to be low so that particles enter one by one into the computation domain. Particles follow the flow streamlines under creeping flow conditions from a random initial location until they are subjected to physico-chemical interactions of DLVO type (15) near the filter surface or a particle already deposited. The computational domain consists of two regions: a fluid region and a porous medium region, i.e. the particle cake. The flow over the two regions of the Hele Shaw cell is computed using the Darcy model after each particle capture to include the local variations of the permeability field due to the cake formation.

MODEL

Let us consider the filtration of a suspension of non-Brownian, non-buoyant, monosized, spherical particles through a model filter. The distribution of pores at the wall is spatially periodic so that the study can be restricted to a representative unit cell of the system with periodic boundary conditions. The direction of the average flow is perpendicular to the membrane. The particles are supposed to be at low concentration in the fluid so that they arrive one by one at the proximity of the filter surface. Moreover it is

assumed that the particle in motion does not modify significantly the flow field but it changes the shape of the cake once it is captured. Then the flow is recalculated every time a new particle accumulates at the filter surface.

Fluid Flow

Under microfiltration conditions, for aqueous solutions, the flow close to the filter can be supposed to be creeping. Indeed even if the flow is turbulent in the system, there exists a viscous sublayer of a few tenths of a micrometer thick at the proximity of the filter. Therefore in this wall region, the Reynolds number based on the characteristic size of the particle or of the pore (1 μm), the kinematic viscosity of water (10^{-6} m^2 s^{-1}) and the fluid velocity (lower than 1 cm s^{-1}) is always lower than 1. Thus the flow is governed by the Stokes equations since the inertia terms of Navier Stokes equations can be neglected. Moreover the porous media flow is governed by the Darcy equation. In the present paper the domain in which filtration is studied is a Hele Shaw cell to take benefit of the simplicity of the Darcy equation. The Hele Shaw cell is a parallelepiped three dimensional domain of very thin thickness equal to one particle diameter as can be seen in Fig. 1 (r is the particle radius, d is the size of the pore).

Under these conditions, the Darcy equation can be used to calculate the flow in the whole domain, i.e. a two dimensional spatially heterogeneous permeability field $K(\vec{x})$ which includes the fluid region (Hele-Shaw region of initial dimensions L_x and L_y and thickness 2.r,) and the porous region

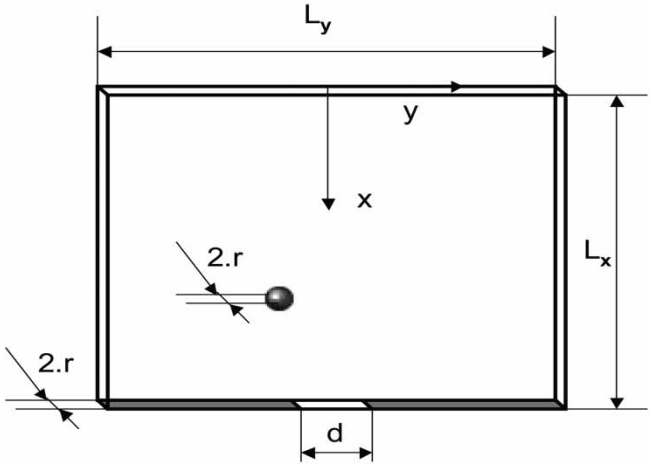

Figure 1. A schematic of the computational domain.

formed by particle accumulation (cake region):

$$\nabla \cdot \vec{u} = 0 \tag{1}$$

$$\vec{u} = -\frac{K(\vec{x})}{\mu}\nabla P \tag{2}$$

μ is the fluid dynamic viscosity, P and $\vec{u}$ are the pressure and velocity of the fluid.

The fluid flow is assumed to be pressure driven, which corresponds to the following boundary conditions:

$$P(0, x) = P_1 \tag{3}$$

$$P\left[|y| < \frac{d}{2}, L_x\right] = P_0 \tag{4}$$

$$\frac{\partial P}{\partial y}\left(\pm\frac{L_y}{2}, x\right) = 0 \tag{5}$$

$$\frac{\partial P}{\partial x}\left(|y| > \frac{d}{2}, L_x\right) = 0 \tag{6}$$

The permeability in the fluid region is that of a Hele Shaw cell of width 2.r:

$$K_{HS} = \frac{(2^{*}r)^2}{12} \tag{7}$$

The permeability in the cake is calculated using the expression proposed by Tsay and Weinbaum (16) according to the particle radius r and the local porosity ε:

$$K_d = K_p\left(1 - \frac{\sqrt{K_p}}{r}\tanh\left[\frac{r}{\sqrt{K_p}}\right]\right) \tag{8}$$

with

$$K_p = 0.0572\, r^2\, \Delta^{2.377} \quad \text{and} \quad \Delta = 2\left[\sqrt{\frac{\pi}{(8/3)(1-\varepsilon)}} - 1\right] \tag{9}$$

Particle Trajectory

Particle trajectories in the domain were obtained from Newton's second law. The particles are assumed to be spherical, monodispersed, non-buoyant, and non-Brownian. The dominant forces, which act on the particles during the formation of the filter cake, are the drag force and the physico-chemical forces. Hence, under the assumption of the absence of inertia which is relevant to the problem, the equation of motion for ith particle can be

written as the simple following force balance:

$$\vec{F}_s^i + \sum_{j=1}^{N_p}\left[\vec{F}_{vdw}^{ij} + \vec{F}_{dl}^{ij}\right] = 0 \tag{10}$$

N_p is the number of particles already captured close to particle "i", F_s, F_{vdw}, and F_{dl} are, respectively, the drag force the attractive Van der Waals force and the repulsive double layer force.

The drag force due to viscous friction acts on every particle. Here it is assumed to be equal to Stokes force. It means that the hydrodynamic interactions, i.e. viscous repulsion due to wall effects, are neglected, so that no correction factors are added to the well-known Stokes force:

$$\vec{F}_s = 6\,\pi\,\mu\,r(\vec{u}_p - \vec{u}) \tag{11}$$

$\vec{u}_p$ is the particle velocity.

For a spherical particle of radius r_i, the Van der Waals force on the ith particle is given by Israelachvili (13). For the separation distance between particles smaller than the particle radius, the Van der Waals potential can be simplified to:

$$V_{vdw} = -\frac{A\,r}{12h} \tag{12}$$

A is the Hamaker constant, h the particle separation distance.

A great number of expressions are proposed in the literature for the double layer force (15) (17). Due to the great number of parameters which appear in the expressions of double layer force in the literature, a simplified expression with two parameters is used for convenience with the corresponding double layer potential between two surfaces is:

$$V_{dl} = B\exp(-\kappa h) \tag{13}$$

where B denotes an energy and κ the Debye-Huckel reciprocal length.

Finally, the problem is formulated in terms of dimensionless variables. Taking L_y as the characteristic length and the Hele Shaw velocity (U_{HS}) as the characteristic velocity, the dimensionless variables can be expressed as:

$$\begin{aligned}
&x^* = \frac{x}{L_y}, \quad y^* = \frac{y}{L_y}, \quad u^* = \frac{u}{U_{HS}}, \quad v^* = \frac{v}{U_{HS}} \\
&L_x^* = \frac{L_x}{L_y}, \quad d^* = \frac{d}{L_y}, \quad r^* = \frac{r}{L_y}, \quad K^* = \frac{K}{L_{yr}}, \quad P^* = \frac{P - P_0}{\rho U_{HS}^2} \\
&A^* = \frac{A}{\rho U_{HS}^2 \cdot L_y^2 \cdot r}, \quad B^* = \frac{B}{\rho U_{HS}^2 \cdot L_y \cdot r^2}, \quad \kappa^* = \kappa \cdot L_y
\end{aligned} \tag{14}$$

with:

$$U_{HS} = \frac{K_{HS}}{\mu}\frac{P_1 - P_0}{L_y} \tag{15}$$

The governing equations for particle trajectory, expressed in dimensionless form where the '*' are omitted, become

$$\frac{d\vec{x}_p}{dt} = \vec{u}_p \tag{16}$$

in which $\vec{u}_p$ is determined from equation (10).

Algorithm of Cake Formation of Particles

Firstly, the Darcy flow governed by equations (1–7) is solved using a finite volume method. Secondly, a particle is launched at a velocity equal to the fluid velocity from a random initial location at the upstream edge of the domain. It moves through the domain following a trajectory which takes account of both the structure of the flow and the physicochemical interactions with the walls, i.e. the filter or the particles already captured, (equations (10–13) and (16) until it makes contact with the filter or a particle already captured or it passes through the pore. If the particle is captured, the permeability field is modified to account for the change in cake geometry. The permeability field is computed from equations (7–9) in a permeability K-mesh which size is equal to particle size. The porosity of each elementary cell is calculated as shown in Fig. 2. The flow field is computed in a more refined F-mesh than K-mesh (typically three times). Once the permeability field is determined, the flow is then recalculated and another particle is launched in the domain. The procedure is repeated until the number of deposited particles fixed at the beginning of simulation is reached.

RESULTS OF SIMULATION

A great number of cakes (100 independent cakes, typically) were simulated in order to give some statistically representative quantitative results. The permeability reduction of the system "model filter and cake" was determined as a function of the volume of particles injected. In the present computation, the particle diameter was chosen between two and four times lower than the pore size. In order to keep the same volume of particles, 29, 100, or 237 particles of diameter two, three and four times lower than the pore, respectively, were injected in each simulation. In addition for all the simulations, the surface porosity is 10% and the dimensionless Hamaker constant is kept equal to 10^{-7}.

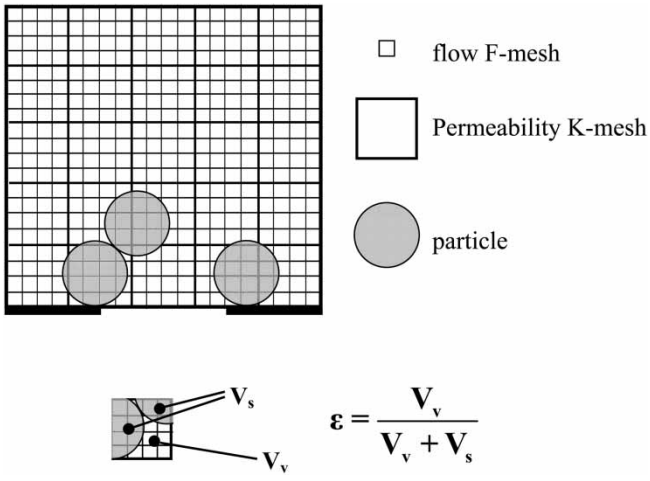

Figure 2. Scheme of permeability K-mesh and fluid flow F-mesh. Detail of porosity calculation within an elementary K-mesh.

Effect of Particle Size

The microstructure of the cakes varies as a function of the model parameters, i.e. attractive or repulsive effects and overall pressure drop in the system.

Existence of Attractive Effects

In this section, it is assumed that the ionic strength is high so that attractive effects dominate. Moreover the overall pressure drop is low. With respect to DLVO approach (Fig. 4), for a high ionic strength the interaction potential is attractive and the increase in the particle size decreases the Debye-Huckel reciprocal length which increases the attractive effect due to the Van Der Waals potential. Thus, the moving particle adheres as soon as it approaches a surface (wall or particle already deposited). Figure 3 exemplifies the effect of particle size on the morphology of the obtained cake.

For each simulation, a certain number of particles captured is needed to produce the partial blockage of the pore and subsequent permeability reduction (Fig. 3). Therefore at the first step of filtration, the permeability is higher when the particle size is high for the same volume of particles deposited (Fig. 5). At the second step of filtration, the effect of particle size is very weak. Dendritic shapes can be observed in the cake. These very porous structures have a low contribution to viscous friction. As a consequence the permeability slowly diminishes and it is almost independent of particle size.

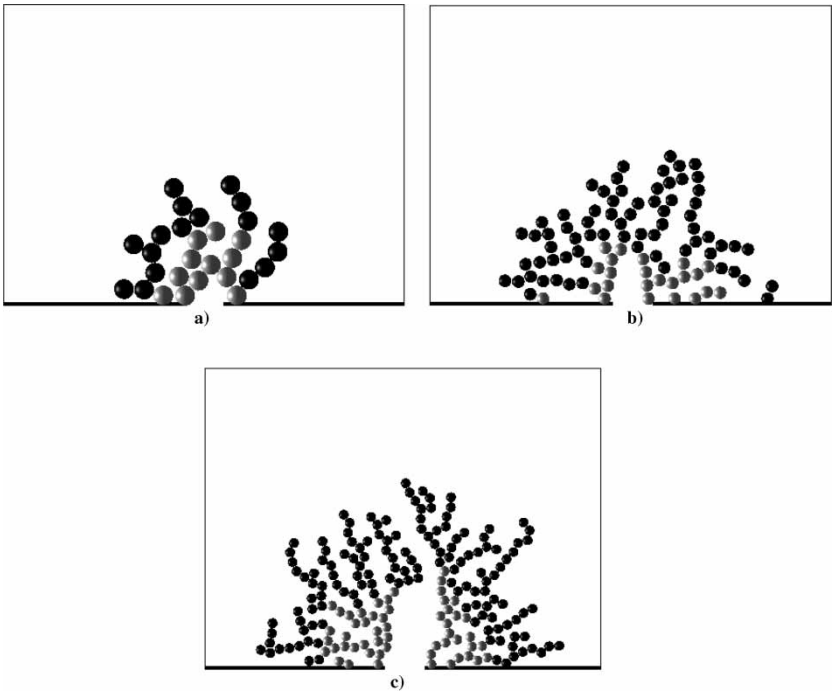

Figure 3. Examples of the particles cakes: $A = 10^{-7}$, $P_1 - P_0 = 1$; a) $r = d/4$ ($Np = 29$, $B = 2.25\ 10^{-10}$, $\kappa = 0.4$); b) $r = d/6$ ($Np = 100$, $B = 2.25\ 10^{-10}$, $\kappa = 0.6$); c) $r = d/8$ ($Np = 237$, $B = 2.25\ 10^{-10}$, $\kappa = 0.8$).

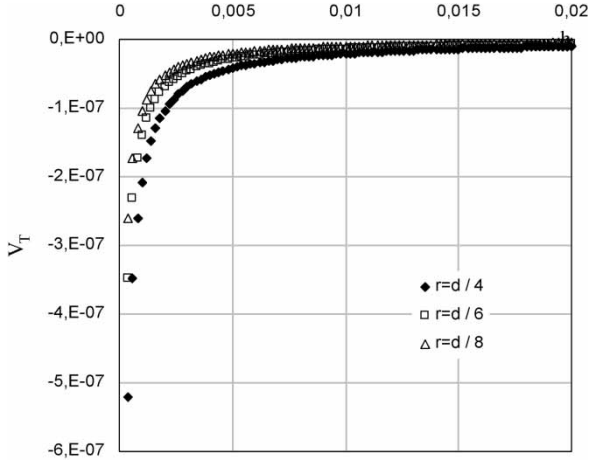

Figure 4. Potential of interaction as a function of the separation distance h used for the study of attractive effects.

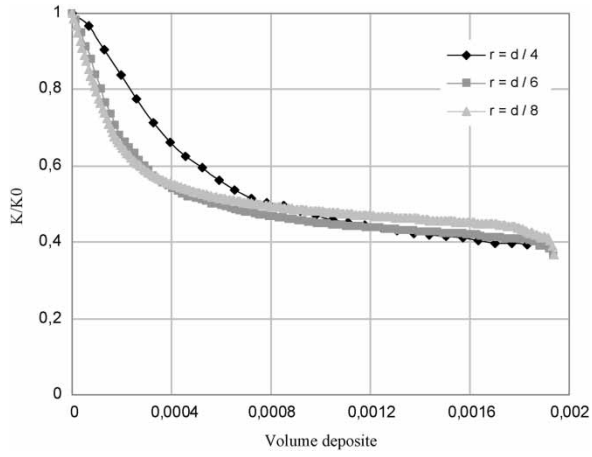

Figure 5. Evolution of the hydraulic conductivity of the system "porous surface and cake" as a function of the volume deposited in the presence of attractive effects.

Existence of Repulsive Effects

Here it is assumed that the ionic strength is weak so that repulsive effects between particles dominate. The corresponding interaction potential is plotted in Fig. 7. In addition the overall pressure drop is kept low. The results presented in Fig. 6 illustrate the effect of particle size on the morphology of the cake for dominant repulsive effects. It can be noticed that particles tend to accumulate close to the pore. An analogue result was previously obtained by Tung et al. (18). The authors have demonstrated that the smaller particles formed a bridge over the pore in particular when the filtration velocity was low. In the present model, the first particles deposited progressively form a bridge over the pore that prevents other particles from passing through it. As can be expected, the bridge is more rapidly built by larger particles. Once the bridge is built, particles are captured when they find a stable position at a distance from other particles according to the potential barrier. The cake grows from the pore bridging and progressively extends with a roughly semi-circular shape throughout the domain.

Figure 8 shows the effect of particle size on the evolution of the permeability of the system "porous surfaces and cake" as a function of the volume deposited. First, it can be noticed that the shape of permeability curves remains the same in every case. However, a significant gap between the curves for the various particle sizes is clearly obtained. It can be observed in Fig. 6 that both the microstructure and the shape of the cake is almost the same for each particle size and in particular the porosity of the cake looks like the same. As a consequence the gap between the curves of Fig. 8 is only due to the difference in terms of particle size. It can also be noticed from

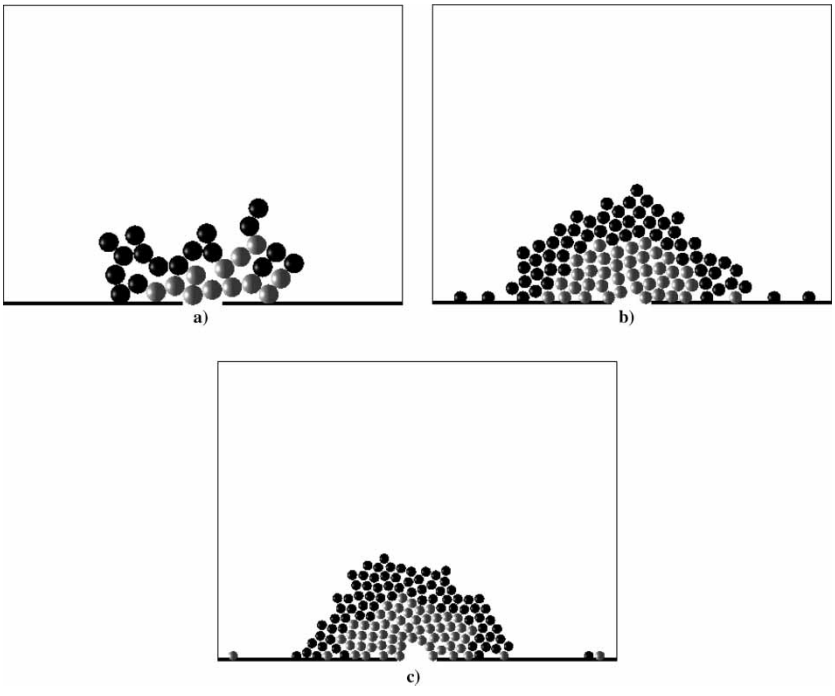

Figure 6. Examples of the particles cakes: $A = 10^{-7}$, $P_1 - P_0 = 1$; a) $r = d/4$ ($Np = 29$, $B = 1.076\ 10^{-6}$, $\kappa = 1023$); b) $r = d/6$ ($Np = 100$, $B = 1.076\ 10^{-6}$, $\kappa = 1535$); c) $r = d/8$ ($Np = 237$, $B = 1.076\ 10^{-6}$, $\kappa = 2046$).

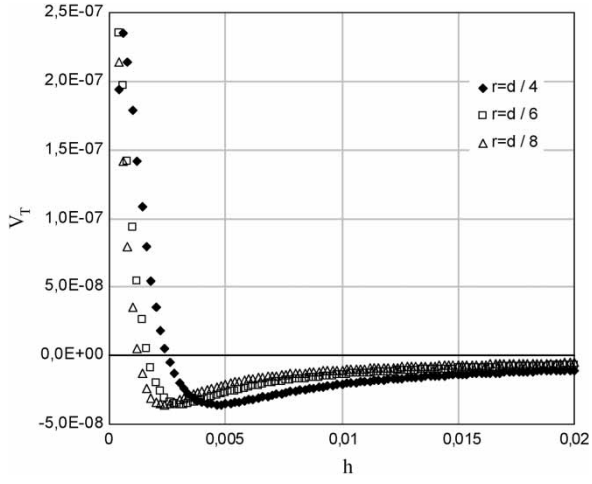

Figure 7. Potential of interaction as a function of the separation distance h used for the study of repulsive effects.

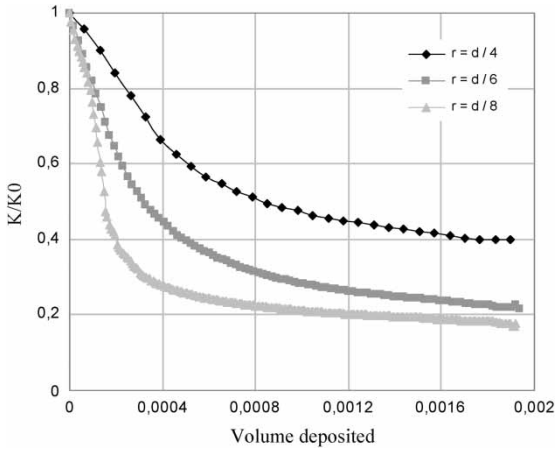

Figure 8. Evolution of the hydraulic conductivity of the system "porous surface and cake" as a function of the volume deposited in the presence of repulsive effects.

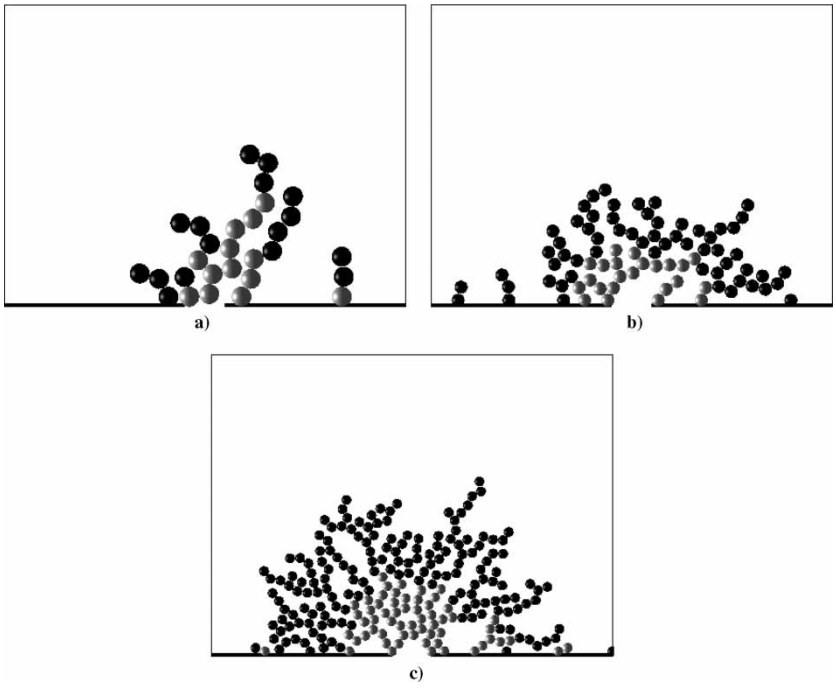

Figure 9. Examples of the particles cakes: $A = 10^{-7}$, $P_1 - P_0 = 100$; a) $r = d/4$ ($Np = 29$, $B = 1.076\ 10^{-6}$, $\kappa = 1023$); b) $r = d/6$ ($Np = 100$, $B = 1.076\ 10^{-6}$, $\kappa = 1535$); c) $r = d/8$ ($Np = 237$, $B = 1.076\ 10^{-6}$, $\kappa = 2046$).

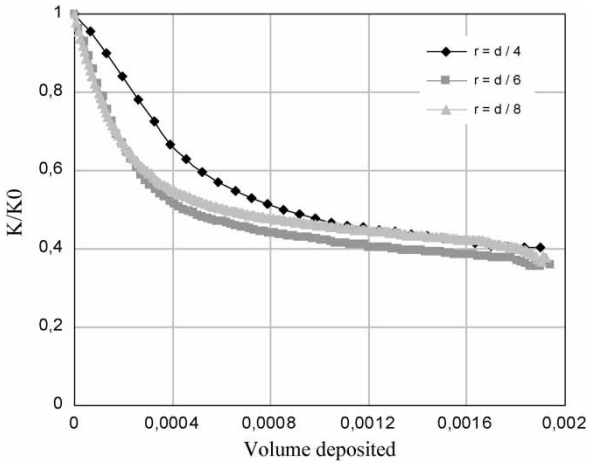

Figure 10. Evolution of the hydraulic conductivity of the system "porous surface and cake" as a function of the volume deposited in presence of high TMP.

Fig. 6 that the bigger the particles the easier the pores can be bridged. However pore bridging occurs for about the same volume of particles. That is why the shape of the permeability reduction curves are roughly the same.

Effect of Overall Pressure Drop

Keeping the same physico-chemical interactions as those of the previous section, the overall pressure drop was increased to study the effect of high

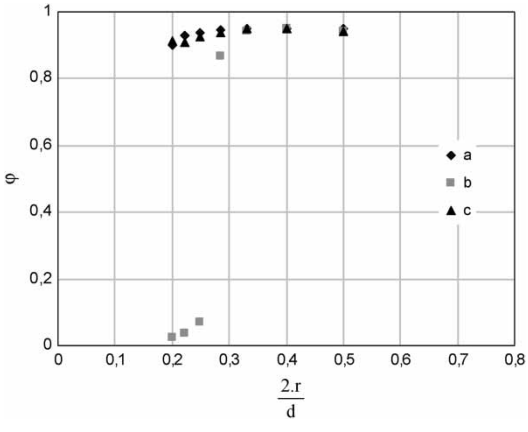

Figure 11. Evolution of capture efficiency of the filter system as a function of particle size for different conditions: a) high ionic strength, b) low ionic strength, c) case b) low ionic strength with high TMP.

viscous friction on the cake microstructure and subsequent permeability reduction of the system. As can be expected the increase of the hydrodynamic force exerted on the particle changes the balance of forces on moving particle (equation (10)). Thus the potential barrier due to weak ionic strength can be overcome so that particle can easily make contact with already aggregated particles and be finally captured. Therefore the cake obtained is less dense. It is almost the same as the one formed when attractive effects dominate but it is more spread out over the wall (Fig. 9). As can be seen in Fig. 10, results in terms of permeability reduction are also comparable with the results of section on the existence of attractive effects.

Capture Efficiency

One of the essential parameters to be quantified for a filter is the capture efficiency:

$$\phi = \frac{N_{pc}}{N_{pc} + N_{pp}}$$

N_{pc}: is the number of particles captured.
N_{pp}: is the number of particles not captured.

The surface porosity is 10% and the Hamaker constant is always the same. The particle sizes selected are $r = d/4$, $d/6$, $d/8$, and $d/10$. The results are interpreted, starting from a statistical study undertaken on a statistically representative number of cakes (100 independent cakes typically), in term of variations of the capture efficiency as a function of the ratio of particle diameter to the pore size. Each simulation corresponds to 100 particles arriving one by one in the calculation field. Figure 11 shows that in the presence of high ionic strength (dominant attractive effects) or high overall pressure drop, the capture efficiency is high and tends towards that for relatively low ratio of particle diameter to pore size. In fact, as it was already discussed in the previous section, the increase of the attractive effects promotes a very open cake structure as the moving particles adhere as soon as they approach a surface (wall or particle already deposited), thus the number of particles that settle on an obstacle is important. On the contrary, for dominant repulsive effects and without high viscous friction, almost all the particles pass through the pore as soon as the ratio of particle diameter to pore size is lower than 0.3 (see Fig. 11). Indeed, repulsive effects prevent particles from approaching the walls thus facilitates their passage through the pore if the particle diameter is relatively smaller than the pore size.

For a better understanding of the phenomenon of cake formation in the presence of repulsive effects between particles, the histograms of the number of realizations as a function of the capture efficiency for different particle diameters is plotted in Fig. 12. It can be shown that for a particle

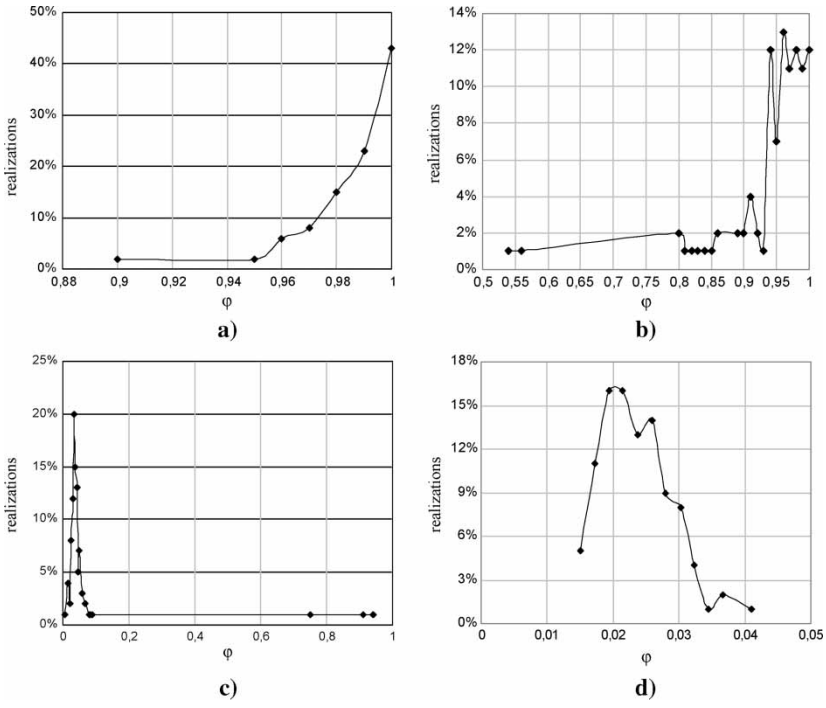

Figure 12. Variation of the percentage of realisations as a function of capture efficiency in presence of repulsive effects: a) $r/d = 4$, b) $r/d = 6$, c) $r/d = 8$, d) $r/d = 10$.

diameter half that of the pore size (case a), the capture efficiency varies between 0.9 and 1. Moreover 43 percents of realizations exhibit a capture efficiency of about 1.

By decreasing the particle size (case b), the repulsive effects increase the percentage of passages of particles through the pore, which involves a significant reduction of the capture efficiency. For case c and case d which correspond to small particle diameters, almost all of realizations have a low capture efficiency ranging between 0.01 and 0.1. Nevertheless for $r/d = 8$, a singular situation having a capture efficiency equal to one can occur. Indeed, when the filtration velocity is low, even very small particles can sometimes form a bridge over the pore to prevent other particles from passing through it.

CONCLUSION

Particle deposition at the filter surface in microfiltration is studied to better understand the effect of particle size on cake morphology and permeability

reduction. Numerical simulations are carried out on a Hele Shaw cell which consists of a representative unit element of a two-dimensional spatially periodic flat plate with pores. It is found that particle size could have a significant effect on particle capture, cake morphology, and subsequent permeability reduction of the filter system depending on hydrodynamic and physicochemical interactions. Such simulations should give new insights on both fouling mechanisms and filtrate flux decline in microfiltration. Further investigations using a three dimensional model and experiments using a a microsieve should confirm and validate the present results.

REFERENCES

1. Benkahla, Y.K., Oul-Dris, A., Jaffrin, M.Y., and Si-Hassen, D. (1995) Cake growth mechanism in cross-flow microfiltration of mineral suspensions. *J. Membr. Sci.*, 98: 107.
2. Huisman, I.H., Elzo, D., Middlelink, E., and Trägardh, A.C. (1998) Properties of the cake layer formed during cross-flow microfiltration. *Colloids Surf.*, 138: 265.
3. Hwang, K.J., Hsu, Y.L., and Tung, K.L. (2006) Effect of particle size on the performance of cross-flow microfiltration. *Advanced Powder Technol.*, 17 (2): 189.
4. Tarabara, V.V., Hovinga, R.M., and Wiesner, M.R. (2002) Constant transmembrane pressure vs. constant permeate flux: effect of particle size on crossflow membrane filtration. *Environ. Eng. Sci.*, 19 (6): 343.
5. Song, L. and Elimelech, M. (1995) Particle deposition onto a permeate surface in laminar flow. *J. Colloid Interf. Sci.*, 173: 165.
6. Kleinstrauer, C. and Chin, T.P. (1984) Analysis of multiple trajectories and deposition layer growth in porous conduits. *Chem. Eng. Commun.*, 28: 193.
7. Hung, C.C. and Tien, C. (1976) Effect of particle deposition on the reduction of water flux in reverse osmosis. *Desalination*, 18: 173.
8. Schmitz, P., Wandelt, B., Houi, D., and Hildenbrand, M. (1993) Description of particle aggregation at the membrane surface in cross-flow microfiltration. *J. Membr. Sci.*, 84: 171.
9. Frey, J.M. and Schmitz, P. (2000) Particle transport and capture at the membrane surface in cross-flow microfiltration. *Chem. Eng. Sci.*, 55: 4053.
10. Seminario, L., Rozas, R., Borquez, R., and Toledo, P.G. (2002) Pore blocking and permeability reduction in cross-flow microfiltration. *J. Membr. Sci.*, 209: 121.
11. Chang, J.S., Tsai, L.J., and Vigneswaran, S. (1996) Experimental investigation of the effect of particle size distribution of suspended particles on microfiltration. *Wat. Sci. Tech.*, 39: 133.
12. Dufrèche, J., Prat, M., Schmitz, P., and Sherwood, J.D. (2002) On the apparent permeability of a porous layer backed by a perforated plate. *Chemical Engineering Science*, 57: 2933.
13. Dufreche, J., Prat, M., and Schmitz, P. (2003) A two-scale domain decomposition method for computing the flow through a porous layer limited by a perforated plate. *Int. Journal for Numerical Methods in Fluids*: 42–623.
14. Noel, F., Schmitz, P., and Prat, M. (2007) Modélisation de la formation d'une couche de particules sur une paroi poreuse, *Congrès Français de Mécanique*.
15. Israelachvili, J. (1985) *Intermolecular and Surface Forces*; Academic Press.

16. Tsay, R. and Weinbaum, S. (1991) Viscous flow in a channel with periodic cross-bridging fibers: exact solutions and Brinkman approximation. *Journal of Fluid Mechanics*, 226: 125.
17. Elimelech, M., Gregory, J., Jia, X., and Williams, R. (1995) *Particle Deposition and Aggregation*; Butterworth Heinemann Ltd.
18. Tung, K.L. and Chuang, C.J. (2002) Effect of pore morphology on fluid flow and particle deposition on track-etched polycarbonate membrane. *Desalination*, 146: 129.